

Motion Generation Using Bilateral Control-Based Imitation Learning with Autoregressive Learning

Ayumu Sasagawa¹, Sho Sakaino², and Toshiaki Tsuji³

Abstract—Robots that can execute various tasks automatically on behalf of humans are becoming an increasingly important focus of research in the field of robotics. Imitation learning has been studied as an efficient and high-performance method, and imitation learning based on bilateral control has been proposed as a method that can realize fast motion. However, because this method cannot implement autoregressive learning, this method may not generate desirable long-term behavior. Therefore, in this paper, we propose a method of autoregressive learning for bilateral control-based imitation learning. A new neural network model for implementing autoregressive learning is proposed. In this study, three types of experiments are conducted to verify the effectiveness of the proposed method. The performance is improved compared to conventional approaches; the proposed method has the highest rate of success. Owing to the structure and autoregressive learning of the proposed model, the proposed method can generate the desirable motion for successful tasks and have a high generalization ability for environmental changes.

I. INTRODUCTION

Robots that can execute various tasks automatically instead of humans are becoming an increasingly important focus of research in the field of robotics. Approaches based on end-to-end learning for motion generation have recently achieved a high performance [1]–[4]. Approach based on reinforcement learning requires a lot of trials [2]. End-to-end learning reduces the effort required for programming, and complex robotic motion can be easily generated. Moreover, they are known as methods having a high generalization ability for situation changes. Among them, “imitation learning (IL)” and “learning from demonstration (LfD)” have attracted attention as methods for efficiently learning robot motion [5]–[10]. They are learning-based methods using the dataset collected through human demonstrations. Yang *et al.* realized autonomous robot operations using neural network (NN) models [9]. Also, a method that combines reinforcement learning and imitation learning was proposed [10]. In addition, IL using force information has been proposed [11]–[17]. Force control improves the robustness against position fluctuations. Therefore, force control raises the possibility of adapting to complex tasks requiring force information and

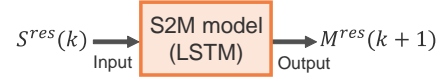


Fig. 1. Network model of our bilateral control-based IL.

realizing more various tasks. [11][12] used haptic devices to collect force information during the demonstrations. Roza *et al.* realized cooperative work between a human and a robot using a Gaussian mixture model (GMM) [13], and Ochi *et al.* used NN models to integrate visual, position, and force information to perform tasks [15]. Also, [17] used Dynamic Movement Primitives (DMP) to model the human demonstrations and realized a task to write letters. A common problem with these approaches is that robot motion was extremely slow compared to humans.

We previously proposed a bilateral control-based IL as one of the methods using force information [18][19]. Bilateral control is a remote-control system that uses two robots, a master and a slave [20][21]. During human demonstrations applying this method, bilateral control was used. A human operated the master, and the slave was teleoperated and conducted tasks within the workspace. In addition, as shown in Fig. 1, the NN model for motion generation predicted the master state from the slave state. The NN model included long short-term memory (LSTM) [22] to predict sequence data. Here, S and M represent the slave and master, respectively. The superscript *res* indicates the response values. In addition, k represents the step of the sequence data. Our bilateral control-based IL can execute tasks requiring a force adjustment and realize fast motion that a conventional IL [11]–[17] cannot realize. Details regarding the advantages of this method are described in Section III.

Although our bilateral control-based IL can achieve a fast and dynamic motion, there is a drawback. The learning method of this approach was unsuitable for a long-term prediction because the NN model was trained based only on a one-step error; this learning method is called teacher forcing [23]. When the NN model is trained using teacher forcing, if prediction errors occur during the prediction process, the errors will accumulate and the robot will not realize a desirable behavior. Autoregressive learning is a method to solve this problem, and the output at the previous step is input to the model in the next step; the method is called free running [24]. Because autoregressive learning predicts a series of motions continuously, the model is learned to minimize the total errors of the long-term prediction. As a result, the model is expected to generate a series of desirable long-term behaviors. To implement autoregressive learning,

¹Ayumu Sasagawa is a student with the Graduate School of Science and Engineering, Saitama University, 255 Shimo-Okubo, Sakura-ku, Saitama City, Saitama 338-8570, Japan. email: a.sasagawa.997@ms.saitama-u.ac.jp

²Sho Sakaino is with the Department of Intelligent Interactive Systems, University of Tsukuba, 1-1-1 Tennodai, Tsukuba, Ibaraki 305-8577, Japan and the JST PRESTO. email: sakaino@iit.tsukuba.ac.jp

³Toshiaki Tsuji is with the Graduate School of Science and Engineering, Saitama University, 255 Shimo-Okubo, Sakura-ku, Saitama City, Saitama 338-8570, Japan. email: tsuji@ees.saitama-u.ac.jp



Fig. 2. Robot (Touch™ USB).

the input and output of the model must be the same variables. In general, the implementation of autoregressive learning is simple [25] because the input and output of the model are the same variables, *i.e.*, response values. By contrast, in our bilateral control-based IL, the output of the model cannot be used as the next input because the input and output of the model are different variables, *i.e.*, the response values of the slave, and the response values of the master (Fig. 1). Therefore, we propose a model in which the input and output of the proposed model have both master and slave response values to implement autoregressive learning in a bilateral control-based IL.

In this study, the proposed model was compared with the conventional models. During the experiments, three tasks were conducted to clarify the effectiveness of the proposed method. The success rates of the tasks were used to evaluate the performance. During all experiments, the proposed method showed an excellent performance equal to or greater than that of previous conventional methods. As mentioned above, our bilateral control-based IL is a method used to solve the issues of conventional ILs [11]–[17]. Owing to the proposed method for autoregressive learning, the bilateral control-based IL achieved a higher performance and success rate. Therefore, this study provides a significant contribution to the field of IL.

The remainder of this paper is organized as follows. Section II introduces the control system and bilateral control. Section III describes the method and advantages of the bilateral control-based IL. Section IV then describes the NN models for the proposed method and previous conventional methods. Section V describes the experiments and presents the results of the three tasks. Section VI provide some concluding remarks regarding this study and discusses areas of future research.

II. CONTROL SYSTEM

A. Robot

Two Touch™ USBs, which are haptic devices manufactured by 3D Systems, were used in the experiments. The two robots were used as the master and slave robots, respectively. The robots have three-degrees-of-freedom (DOF), as shown in Fig. 2. The robots can measure only the joint angles θ_1 , θ_2 , and θ_3 with the encoders. Here, the subscripted numbers represent each joint shown in Fig. 2.

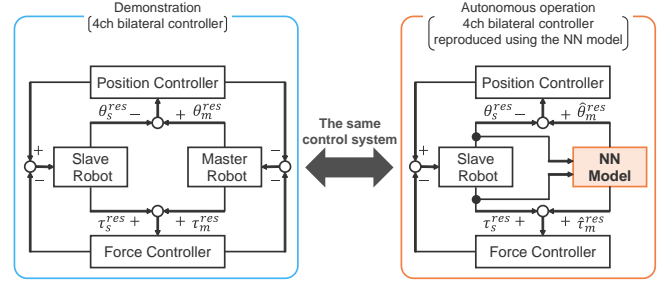


Fig. 3. 4ch bilateral controllers during the demonstrations and the autonomous operation. The figure on the left side shows a 4ch bilateral controller during the demonstrations. As shown on the right side of the figure, the master is replaced with the NN model to reproduce the 4ch bilateral controller during an autonomous operation. With the method proposed in this paper, the master response values are input to the NN model in addition to the slave response values. The same control system is applied during the demonstration and autonomous operation.

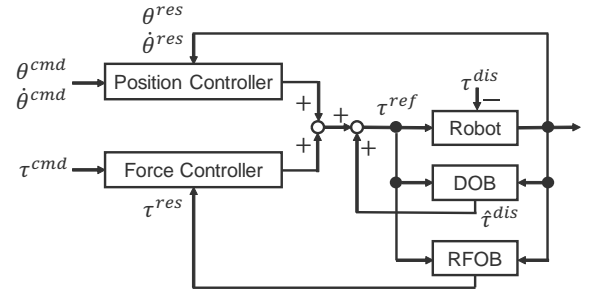


Fig. 4. Controller.

B. Bilateral control

Bilateral control is a remote control system that uses two robots, a master and a slave [20][21]. In this study, 4ch bilateral control [26][27] was used from among various types of bilateral control because the 4ch bilateral control has the highest performance and an excellent operability, and the slave and master consist of both position and force controllers. Therefore, 4ch bilateral control is suitable for IL [19]. In bilateral control, when the operator operates the master, the slave is teleoperated. The control goal is to synchronize the position and satisfy the law of action and reaction forces between the two robots. The reaction force caused by the contact between the slave and the environment is presented to the master. Thus, the operator can feel the interactions between the slave and the environment. The control law of 4ch bilateral control is expressed through the following equations using the angle response values θ^{res} and the torque response values τ^{res} of the robots. The block diagram is expressed on the left side of Fig. 3. In addition, the subscripts s and m represent the slave and master, respectively, and the superscript res represents the response values.

$$\theta_m^{res} - \theta_s^{res} = 0, \quad (1)$$

$$\tau_m^{res} + \tau_s^{res} = 0. \quad (2)$$

C. Controller

The control system consisted of position and force controllers, as shown in Fig. 4. Here, θ , $\dot{\theta}$, and τ represent

TABLE I
GAINS AND IDENTIFIED SYSTEM PARAMETERS
FOR ROBOT CONTROLLER

	Parameter	Value
J_1	inertia (θ_1) [mkgm ²]	2.55
J_2	inertia (θ_2) [mkgm ²]	4.30
J_3	inertia (θ_3) [mkgm ²]	1.12
G_1	Gravity compensation coefficient 1 [mNm]	79.0
G_2	Gravity compensation coefficient 2 [mNm]	55.0
G_3	Gravity compensation coefficient 3 [mNm]	33.0
D	Friction compensation coefficient [mkgm ² /s]	4.55
K_p	Position feedback gain	121
K_d	Velocity feedback gain	22.0
K_f	Force feedback gain	1.00
g	Cut-off frequency of pseudo differentiation [rad/s]	40.0
g_{DOB}	Cut-off frequency of DOB [rad/s]	40.0
g_{RFOB}	Cut-off frequency of RFOB [rad/s]	40.0

the joint angles, angular velocity, and torque of each joint, respectively. The superscripts *res*, *cmd*, and *ref* indicate the response, command, and reference values, respectively. In addition, θ^{res} was measured by the encoders of the robots, and $\dot{\theta}^{res}$ was calculated using a pseudo-differentiation. The disturbance torque τ^{dis} was estimated by a disturbance observer (DOB) [28] as $\hat{\tau}^{dis}$. Furthermore, a reaction force observer (RFOB) [29] calculated the reaction force τ^{res} . Details of the RFOB are described in Section II-D. The position controller also included a proportional and derivative controller, and the force controller consisted of a proportional controller. The torque reference values τ^{ref} of the slave and master were calculated as follows:

$$\tau_m^{ref} = -\frac{J}{2}(K_p + K_d s)(\theta_m^{res} - \theta_s^{res}) - \frac{1}{2}K_f(\tau_m^{res} + \tau_s^{res}), \quad (3)$$

$$\tau_s^{ref} = \frac{J}{2}(K_p + K_d s)(\theta_m^{res} - \theta_s^{res}) - \frac{1}{2}K_f(\tau_m^{res} + \tau_s^{res}), \quad (4)$$

where s represents the Laplace operator. Here, J is the inertia, and K_p , K_d , and K_f represent the position, velocity, and force control gain, respectively. The gain values and cut-off frequency used in the experiments are shown in Table I.

D. The system identification

The following equations represent robot dynamics.

$$J_1 \ddot{\theta}_1^{res} = \tau_1^{ref} - \tau_1^{dis} - D\dot{\theta}_1^{res}, \quad (5)$$

$$J_2 \ddot{\theta}_2^{res} = \tau_2^{ref} - \tau_2^{dis} - G_1 \cos \theta_2^{res} - G_2 \sin \theta_3^{res}, \quad (6)$$

$$J_3 \ddot{\theta}_3^{res} = \tau_3^{ref} - \tau_3^{dis} - G_3 \sin \theta_3^{res}. \quad (7)$$

Here, D and G represent the friction compensation coefficient and gravity compensation coefficient, respectively. The numbers in the subscript represent each joint of the robots. The off-diagonal term of the inertia matrix was ignored because it was negligibly small. The parameters of the control system were identified on the basis of [30]. Friction D and gravity G were identified under free motion, assuming

$\tau^{dis} = 0$. The DOB calculated the estimated disturbance torque $\hat{\tau}^{dis}$ as follows:

$$\hat{\tau}^{dis} = \tau^{ref} - J\ddot{\theta}^{res}. \quad (8)$$

The torque response values of each joint were calculated as follows:

$$\tau_1^{res} = \hat{\tau}_1^{dis} - D\dot{\theta}_1^{res}, \quad (9)$$

$$\tau_2^{res} = \hat{\tau}_2^{dis} - G_1 \cos \theta_2^{res} - G_2 \sin \theta_3^{res}, \quad (10)$$

$$\tau_3^{res} = \hat{\tau}_3^{dis} - G_3 \sin \theta_3^{res}. \quad (11)$$

Each identified parameter used in the experiment is shown in Table I.

III. METHOD AND ADVANTAGE OF BILATERAL CONTROL-BASED IMITATION LEARNING

A. Method

The robots learned behaviors from human demonstrations, and then conducted the tasks autonomously. In the demonstrations, the desired tasks were conducted using 4ch bilateral control. A human operated the master, and the slave performed the tasks in the workspace. The joint angles, angular velocity, and torque response values of the two robots were saved as the dataset for model training. Both the control cycle and the data saving cycle were 1 ms.

Then, the NN model was trained using the dataset collected during the demonstrations. The NN model consisted of LSTM and fully connected layers to learn the time series data. Basically, the model was trained to input the state at time t and output the state at time $t + 20$ ms. Whether the input and output were the master state and/or the slave state depended on each model described in Section IV. The state consisted of the joint angles, angular velocity, and torque response values. The loss function is the mean squared error between the model output values and the true values of the dataset. The model was learned to minimize the loss function. The dataset values were normalized to [0, 1] before the input to the model.

Finally, the trained model generated the motion, and the robot autonomously conducted the tasks. The control system was designed to reproduce 4ch bilateral control during the autonomous operation. The joint angle, angular velocity, and torque response values of the slave were measured in real time and input to the learned model. The command values predicted by the model were normalized before the input to the slave controller. Note that the prediction cycle of the model was 20 ms, whereas the control cycle of the robot was 1 ms.

B. Advantage

The main advantages of bilateral control-based IL are the following two points.

1) *IL using force information can be realized*: Bilateral control-based IL can realize tasks requiring a force adjustment. By using bilateral control, force information can be collected during the demonstrations. The master measures the operator's action force, and the slave measures the reaction

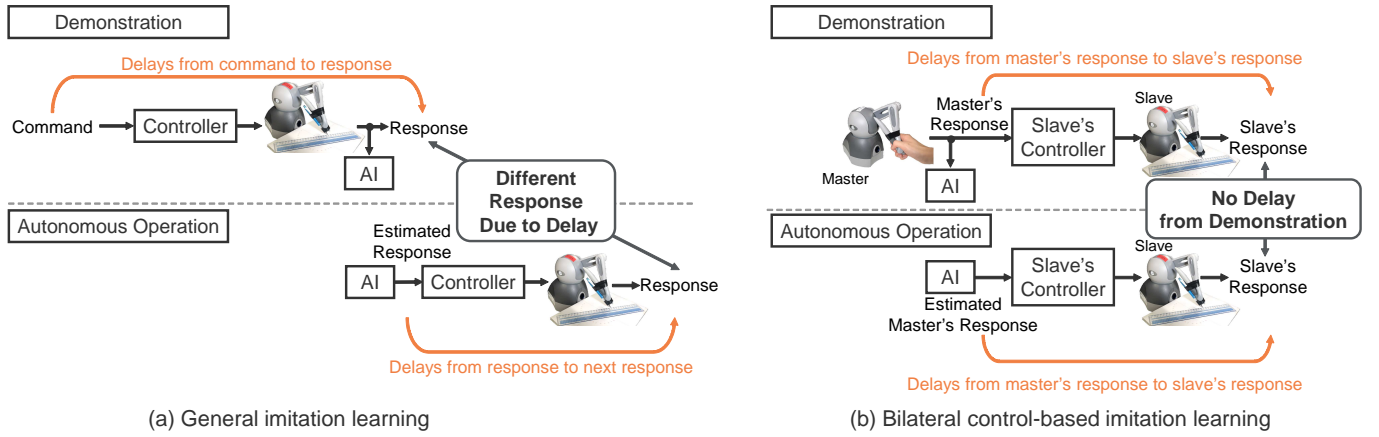


Fig. 5. Overview of general IL and our bilateral control-based IL. In general, the delays caused during the demonstration and autonomous operation are different. Therefore, a general IL can realize only slow motion, which can ignore delays. In the bilateral control-based IL, the delays caused during the demonstration and autonomous operation are the same. Thus, in our bilateral control-based IL, fast motion with delays can be achieved.

force from the environment. When using the RFOB, each force can be measured without a force sensor.

2) *Fast motion can be realized:* The most notable advantage of a bilateral control-based IL is that robots can achieve fast motion. One of the common issues of conventional ILs [11]–[17] is that robot motion is extremely slow compared to human motion. As shown in Fig. 5-(a), in general IL, the response values collected during the demonstrations are given as the command values during the autonomous operation because the command values cannot be measured directly during the demonstrations. In robot control, eliminating control delays is virtually impossible. In addition, when performing tasks, including contact with the environment, delays due to physical interactions occur. In general, the robots cannot reproduce the same motion as the demonstrations because of the different delays during the autonomous operation and the demonstrations. For this reason, a general IL can achieve only slow motion and can ignore the delays. From the above, the following two points must be satisfied to realize fast motion in the IL.

- (i) Command values must be predicted during autonomous operation, *i.e.*, the command values must be collected during the demonstrations,
- (ii) The same control system must be implemented during the demonstrations and autonomous operation.

Our bilateral control-based IL can satisfy these two points for the following reasons. First, in bilateral control, the command values of the slave are the response values of the master. Therefore, the command values and the response values of the slave can be measured separately. As a result, the command values of the slave can be predicted during an autonomous operation. As shown in Fig. 5-(b), in our bilateral control-based IL, the delays that occur during the demonstrations similarly occur during the autonomous operation. Second, as shown in Fig. 3, in a bilateral control-based IL, the system is designed to reproduce bilateral control during an autonomous operation. Hence, the control system can be the same during the demonstrations and autonomous

operation. During the demonstrations using bilateral control, humans collect data considering the delays, *i.e.*, humans demonstrate skills to compensate for the delays. If the control system is different during the demonstrations and an autonomous operation, this compensation skill will be lost. However, our bilateral control-based IL can reproduce this skill during an autonomous operation. A bilateral control-based IL can satisfy the above two points, and the method can execute tasks with fast motion performed through bilateral control. Therefore, this is a suitable method for IL because the robot can perform tasks requiring a force adjustment and achieve a fast motion.

IV. NEURAL NETWORK MODEL

A. Autoregressive learning

Fig. 6 shows the LSTM model developed in the time direction. Here, x represents an arbitrary value used for the input and output, and the superscript tr represents the teacher data. In addition, $\hat{\cdot}$ represents the predicted values of the model. Fig. 6-(a) shows the learning method without autoregressive learning. With this method, the teacher data are input at each step during the learning process, that is, the input values were completely unaffected by the prediction in the previous steps. That is, the output error used to train the NN model is based only on a one-step prediction. As shown in Fig. 6-(c), the model's prediction values are used in the prediction process. If prediction errors occur during the prediction process, they will accumulate. Therefore, although the model was learned with high accuracy during the learning process, the model could not generate the desirable behavior during the prediction process. This problem similarly occurs in the field of natural language processing using a recurrent neural network (RNN) [31][32]. By contrast, in the method with autoregressive learning, as shown in Fig. 6-(b), the model's predicted values are used for the input even during the learning process. Because autoregressive learning predicts a series of motions continuously, the model is learned to minimize the total errors of the long-term prediction. As

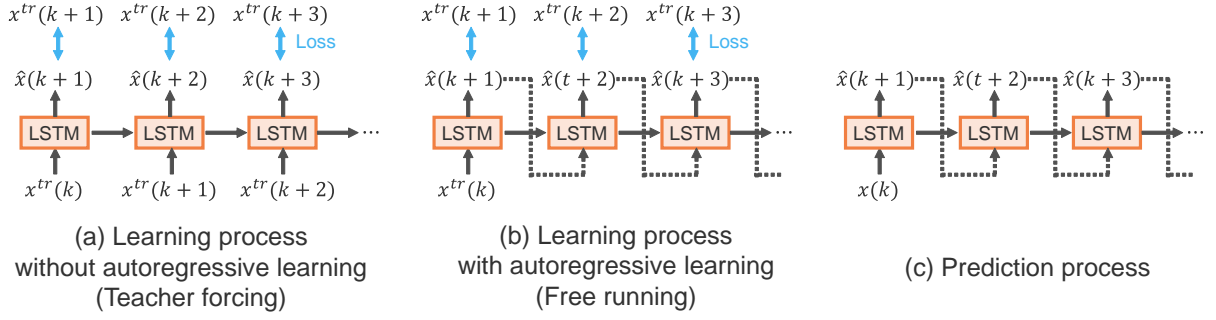


Fig. 6. Learning and prediction method using LSTM with and without autoregressive learning.

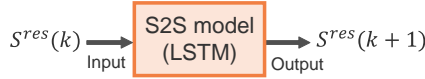


Fig. 7. Network model of the S2S model (conventional method).

a result, the model is more likely to generate the desirable behavior in the long-term to execute the tasks.

In a conventional bilateral control-based IL [18][19], autoregressive learning cannot be implemented. This is because the input and output of the model were different variables, *i.e.*, the slave's response values, and the master's response values (Fig. 1). In this paper, the SM2SM model is proposed to solve this problem. In addition, the performances of three models including the proposed method were compared. The summary of each model is shown in Table II. The general IL [11]–[17] predicted the next response values from the current response values. Therefore, the S2S model that predicts the next slave state from the current slave state was used as a comparison method that replicates the general IL. In addition, the S2M model was used as the conventional bilateral control-based IL [18][19], and the SM2SM model was used as the proposed method. Details of each model are described in the following sections.

B. S2S model (Conventional model)

As shown in Fig. 7, the S2S model predicts the next state of the slave from the current state of the slave. The input and output consisted of the joint angles, angular velocity, and torque response values of the slave with three DOFs, that is, the S2S model had nine inputs and nine outputs.

1) *Learning*: During the learning process, the slave's response values were input, and the slave's response values 20 ms later were output. The S2S model was trained without or with autoregressive learning. The case without autoregressive learning is called S2S-w/o-AR, and the case with autoregressive learning is called S2S-AR. In this study, the number of autoregressive steps was set to 10 to converge the prediction errors quickly. That is, the values of the training dataset were input instead of the predicted values of the previous step for every 10 steps.

2) *Autonomous operation*: The model predicted the response values of the slave. The predicted values of the model were used as the command values of the slave.

C. S2M model (Conventional model)

As shown in Fig. 1, the S2M model predicts the next state of the master from the current state of the slave. The input consisted of the joint angles, angular velocity, and torque response values of the slave with three DOFs. The output was composed of these response values of the master with three DOFs. Therefore, the S2M model had nine inputs and nine outputs.

1) *Learning*: During the training, the response values of the slave were input, and the model output the response values of the master 20 ms after the input was applied. In the case of the S2M model, the model was trained without autoregressive learning because it could not be implemented. The S2M model without autoregressive learning is called S2M-w/o-AR.

2) *Autonomous operation*: The model predicted the response values of the master. The predicted values of the model were used as the command values of the slave.

D. SM2SM model (Proposed model)

SM2SM is the proposed model applied to adapt autoregressive learning to a bilateral control-based IL. As shown in Fig. 8-(a), the SM2SM model predicts the next state of the slave and master from the current state of the slave and master. In contrast to the S2M model, the input and output of the SM2SM model consisted of both the slave and master states. Therefore, autoregressive learning could be implemented. In addition, owing to this structure, the model can better learn the relationship between the slave and master. Because interactions between master and slave robots can be implicitly learned by the SM2SM model, it is expected that the SM2SM model is a suitable model for bilateral control-based IL. The input and output consisted of the joint angles, angular velocity, and torque response values of the slave and master with three DOFs, that is, the SM2SM model had 18 inputs and 18 outputs.

1) *Learning*: An overview of the learning process of this model is shown in Fig. 8-(b). During the learning process, the response values of the slave and master were input, and the response values of the slave and master 20 ms later were output. The SM2SM model was learned without or with autoregressive learning. The case without autoregressive learning is called SM2SM-w/o-AR, and the case with

TABLE II
DETAILS OF NEURAL NETWORK MODEL

Model	Neural network model		Autoregressive learning
	Input	Output	
S2S-w/o-AR	Slave (9 dims.)	Slave (9 dims.)	-
S2S-AR	Slave (9 dims.)	Slave (9 dims.)	✓
S2M-w/o-AR	Slave (9 dims.)	Master (9 dims.)	-
SM2SM-w/o-AR	Slave and master (18 dims.)	Slave and master (18 dims.)	-
SM2SM-AR (Proposed model)	Slave and master (18 dims.)	Slave and master (18 dims.)	✓

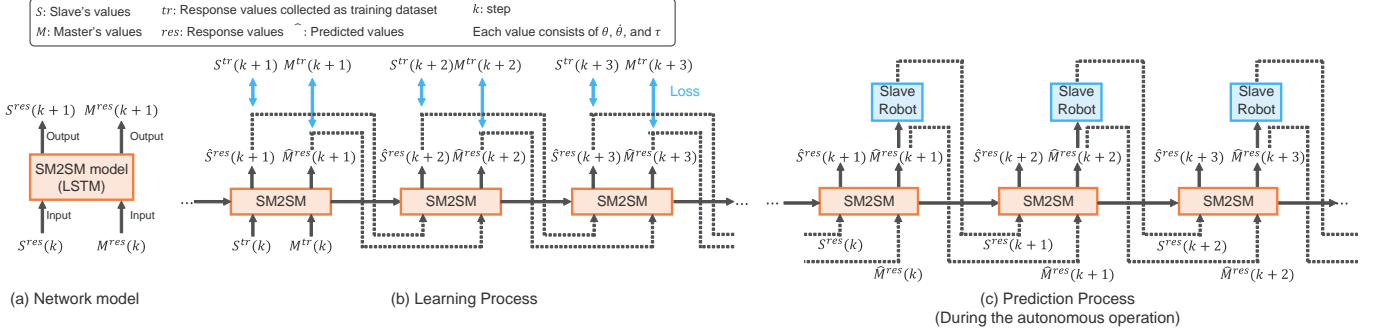


Fig. 8. Learning process and prediction process of the SM2SM model (proposed method).

autoregressive learning is called SM2SM-AR. In this study, the number of autoregressive steps was set to 10 to converge the prediction errors quickly.

2) *Autonomous operation*: Overview during the autonomous operation is shown in Fig. 8-(c). The slave state among the input to the model was the slave response values measured in real time. By contrast, the state of the master among the inputs of the model was that predicted by the model one step before. The states of the master predicted by the model were used as the command values of the slave.

V. EXPERIMENT

During the experiment, three types of tasks were conducted to clarify the effectiveness of the proposed method. Three types of NN models were compared during each experiment. The S2M model was the only model without autoregressive learning, the S2S and SM2SM models were compared with and without autoregressive learning, and five types of models were compared. The success rate of the tasks verified the performance of each model.

A. Experiment 1 (Drawing a line with a pen and a ruler)

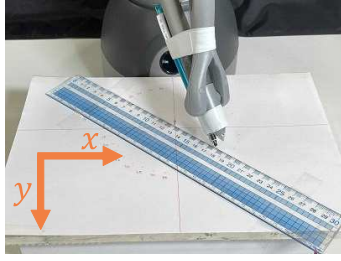
1) *Task design*: Fig. 9-(a) shows the setup of this experiment. A mechanical pencil was fixed to the slave. Initially, the slave moved from the initial position toward the ruler. After touching the ruler, the slave drew a straight line to the right along the ruler. The goal of this task was to draw lines according to various inclinations. As shown in Fig. 10-(a), the inclination was defined by the angle at which the ruler was rotated around the point where the pen first contacted the ruler. Zero degrees is represented by the "reference line" in the figure. To succeed in this task, a proper adjustment of the contact force between the pen and the ruler or paper was required. In addition, adaptability to unknown inclinations or unknown positions of the ruler was required.

2) *Human demonstrations and dataset for learning*: We collected data with ruler inclinations of zero, 20, and 40 degrees, as shown Fig. 10-(a). Eight trials were conducted for each inclination; the total number of trials was 24. One trial time was 3 s. The slave started moving from the initial position and drew a line of 5 cm or longer along the ruler within 3 s.

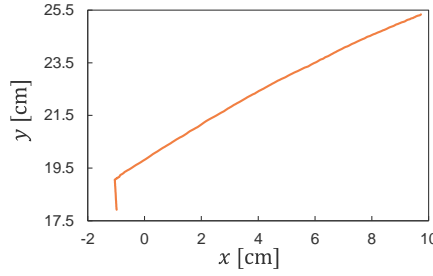
3) *Neural network architecture*: The NN model consisted of six LSTM layers, followed by a fully connected layer. The unit size of all layers was 50. The mini-batch consisted of 100 random sets of 150 time-sequential samples corresponding to 3 s.

4) *Task validation*: To verify the autonomous operation, the performance of the ruler inclinations from -30 to 80 degrees was verified every 10 degrees. Success was defined as the case in which the robot drew a 5 cm or longer line along the ruler. Verification was conducted through three trials for the inclination of each ruler. In addition, the performance when the ruler's position was shifted back and forth was validated. Here, the position of the ruler was defined based on the point where the pen first contacted the ruler. As shown in Fig. 10-(b), the validation was conducted by shifting 0.8 cm back and forth from the learned position. The learned position was "reference line B," and the unlearned positions were "reference line A" and "reference line C."

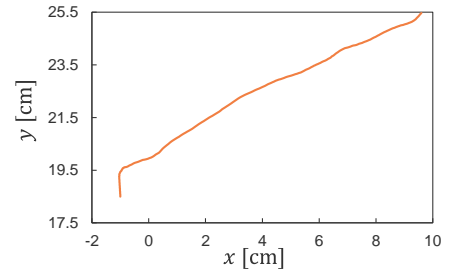
5) *Experimental results*: The success rates of each model are shown in Table III. First, comparing the models without autoregressive learning, S2S-w/o-AR had a higher success rate than S2M-w/o-AR and SM2SM-w/o-AR. As mentioned in Section III, the S2M model was more suitable than the S2S model for IL, including fast motion with delays. However, this task was not particularly fast. In addition, during the drawing task, the motion of the slave was restrained by the ruler. The dataset of the slave's response values was easy to



(a) Setup and defined coordinates

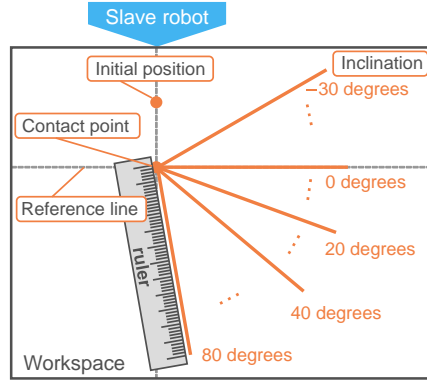


(b) Slave's response value

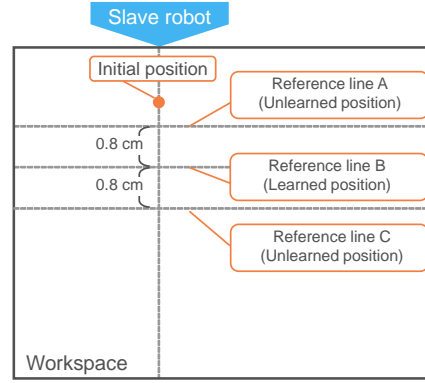


(c) Master's response value

Fig. 9. The setup and the training data of the drawing task when drawing a 40 degree line. The response values of the slave did not include large fluctuations (Fig. b). Compared to that, the response values of the master included large fluctuations (Fig. c).



(a) Outline of the drawing task



(b) Changes in the position of the ruler

Fig. 10. The outline of the drawing task.

TABLE III
SUCCESS RATES OF THE DRAWING TASK

Model	Reference line	Success Rate [%]														Subtotal	Total
		Inclination [deg]															
		−30	−20	−10	0*	10	20*	30	40*	50	60	70	80				
S2S-w/o-AR	A	0	100	100	100	100	100	100	100	100	100	100	100	91.7	88.0 (95/108)		
	B**	0	100	100	100	100	100	100	100	100	100	100	100	91.7			
	C	0	0	100	100	100	100	100	100	100	100	100	66.7	81.0			
S2S-AR	A	0	100	100	100	100	100	100	100	100	100	100	100	91.7	93.5 (101/108)		
	B**	0	100	100	100	100	100	100	100	100	100	100	100	91.7			
	C	100	100	100	100	100	100	100	100	100	100	100	66.7	97.2			
S2M-w/o-AR	A	0	0	0	66.7	100	100	100	100	100	100	100	66.7	69.4	66.7 (72/108)		
	B**	0	0	0	100	100	100	100	100	100	100	66.7	0	63.9			
	C	0	0	0	100	100	100	100	100	100	100	100	0	66.7			
SM2SM-w/o-AR	A	0	0	100	100	100	100	100	100	0	100	100	100	75.0	81.0 (87/108)		
	B**	0	0	100	100	100	100	100	100	100	100	100	100	83.3			
	C	0	0	100	100	100	100	100	100	100	100	100	100	83.3			
SM2SM-AR (Proposed method)	A	100	100	100	100	100	100	100	100	100	100	100	100	100	100 (108/108)		
	B**	100	100	100	100	100	100	100	100	100	100	100	100	100			
	C	100	100	100	100	100	100	100	100	100	100	100	100	100			

*: Learned inclination of the ruler

**: Learned position of the ruler

learn because it did not include large fluctuations, as shown in Fig. 9. By contrast, fluctuations may be contained in the master responses because the master was not restrained by anything, as shown in Fig. 9. Therefore, in the case of using the master responses in the input or output of the model, such as the S2M and SM2SM models, learning was difficult. In addition, SM2SM-w/o-AR showed a higher performance than S2M-w/o-AR. As described in Section IV-D, the structure of the SM2SM model was more suitable than the structure of the S2M model because accurately understanding

the relationship between the master and slave was necessary for bilateral control-based IL.

Furthermore, SM2SM-AR had a higher success rate than SM2SM-w/o-AR and the highest success rate among all models. In particular, compared to other methods, SM2SM-AR had a high adaptability to changes in the ruler's position and extrapolation inclinations. As described in Section IV, autoregressive learning is a method that was evaluated not by the prediction error of only one step, but by the prediction error of all consecutive steps. Therefore, the model can

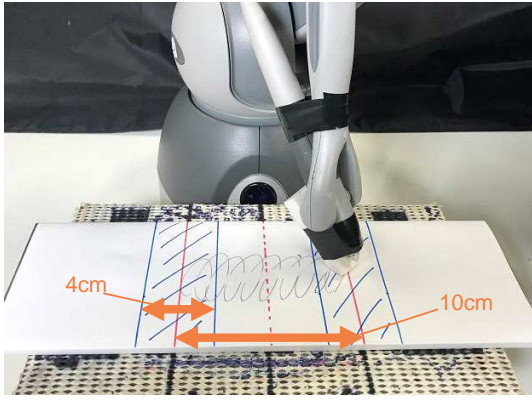


Fig. 11. Experimental setup of the erasing task. During the human demonstrations, the training data were collected to erase the area inside the solid red line. In the verification of the autonomous operation, the success was defined as the case in which the movement was switched in the opposite direction in the area indicated by the blue diagonal line.

properly generate a series of motions to perform a task even for unknown environments, and the effects of the fluctuation of the master's responses were negligible. These results indicate that the proposed model's structure and autoregressive learning improved the generalization performance for unknown environments, even with fluctuating responses. The generalization of the proposed method, which can achieve high success rates even in unknown environments, is expected to be applied to other tasks.

B. Experiment 2 (Erasing a line with an eraser)

1) *Task design*: Fig. 11 shows the setup of this experiment. An eraser was fixed to the slave. The slave erased a line written on the paper with the eraser. The goal of this task was to erase a line according to various paper heights. Adaptability to unknown paper heights was required. To succeed in this task, proper adjustment of the contact force between the eraser and the paper was required. In this task, the robot had to operate fast and utilize the inertial force because a large amount of friction occurred between the eraser and paper.

2) *Human demonstrations and dataset for learning*: We collected data with paper heights of 35, 55, and 75 mm. Five trials were conducted for each paper height, and the total number of trials was 15. One trial time was 10 s. The dataset was collected to erase the area inside the solid red line shown in Fig. 11. The slave moved horizontally in the figure, and the slave repeatedly moved in the opposite direction at the solid red line. The slave robot was teleoperated to reciprocate left and right within the area at approximately constant cycles.

3) *Neural network architecture*: The NN model consisted of two or four LSTM layers, followed by a fully connected layer. During this task, two types of NN architectures were used because the robot behavior differed depending on the number of LSTM layers, and the difference in the architecture affected the results. The unit size of all layers was 50. The mini-batch consisted of 100 random sets of 300 time-sequential samples corresponding to 6 s.

4) *Task Validation*: In verifying the autonomous operation, the performance for paper heights of 35, 45, 55, 65,

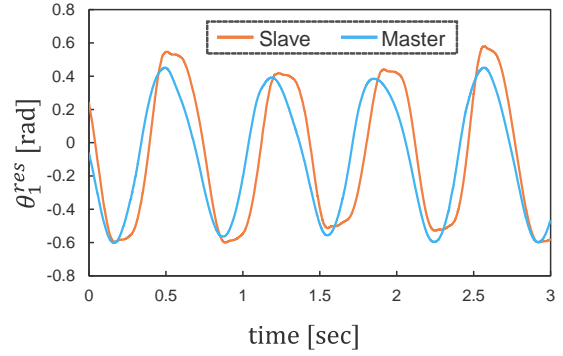


Fig. 12. Training data of the erasing task. The figure shows the response values of joint angle 1 θ_1^{res} for a paper height of 75 mm.

and 75 mm was verified. The paper heights of 45 and 65 mm were the untrained height. Success was defined as the case in which the robot erased the line within the specified area. We defined the area of success to exclude cases in which the robot movements were too narrow or too wide as compared to successful demonstrations. In Fig. 11, when the robot reciprocated to the left and right, the success was the case in which the movement was switched in the opposite direction in the area indicated by the blue diagonal line. Of course, the ability to erase the line with the appropriate force according to the changes in height was an essential condition for success. The robot executed the task for 8 s for each trial, and the case in which the robot stopped during the trial was defined as a failure. Verification was conducted through three trials for each paper height.

5) *Experimental results*: The success rates of each model are shown in Table IV. The rates in the rightmost column of the table were evaluated using a different evaluation criterion instead of the above evaluation criterion. These results show the percentage of the trials in which the robot could continue erasing the line without stopping during the trial, regardless of whether they satisfied the success criteria based on the success area explained above. During this experiment, the results differed owing to the number of LSTM layers. The performance was validated by changing the number of LSTM layers of each model. As shown in the table, the S2S model generally had low success rates. Many of the failures were cases in which the robot stopped owing to friction between the eraser and the paper, or the robot went outside of the workspace. During this task, the robot had to move extremely quickly. In addition, a large amount of friction occurred between the eraser and the paper. Hence, control delays and delays owing to physical interactions occurred during the demonstrations. The angle response values of the training data are shown in Fig. 12. We focused on θ_1^{res} because joint 1 moved mainly during the erasing task. The figure shows that a delay between the response values of the master and slave occurred. Therefore, the skill required to compensate for the delays performed by humans during the demonstrations had to be reproduced during the autonomous operation. The S2S model lost this compensation skill and could not achieve this task requiring fast motion.

By contrast, both the S2M and SM2SM models showed

TABLE IV
SUCCESS RATES OF THE ERASING TASK

Model	The number of LSTM layer	Success rate based on the success area [%]						Total rate of robot continued to perform the task during the trial [%]
		Height [mm]					Total	
		35*	45	55*	65	75*		
S2S-w/o-AR	2	0	0	0	66.7	33.3	20.0 (3/15)	40.0 (6/15)
	4	0	0	0	100	100	40.0 (6/15)	100 (15/15)
S2S-AR	2	33.3	0	0	0	0	6.67 (1/15)	80.0 (12/15)
	4	0	0	0	0	0	0 (0/15)	100 (15/15)
S2M-w/o-AR	2	100	100	66.7	100	100	93.3 (14/15)	100 (15/15)
	4	100	66.7	66.7	100	100	86.7 (13/15)	100 (15/15)
SM2SM-w/o-AR	2	0	0	0	0	33.3	6.67 (1/15)	100 (15/15)
	4	100	66.7	100	100	100	93.3 (14/15)	100 (15/15)
SM2SM-AR (Proposed method)	2	100	100	100	66.7	100	93.3 (14/15)	100 (15/15)
	4	100	100	33.3	66.7	100	80.0 (12/15)	100 (15/15)

*: Learned height

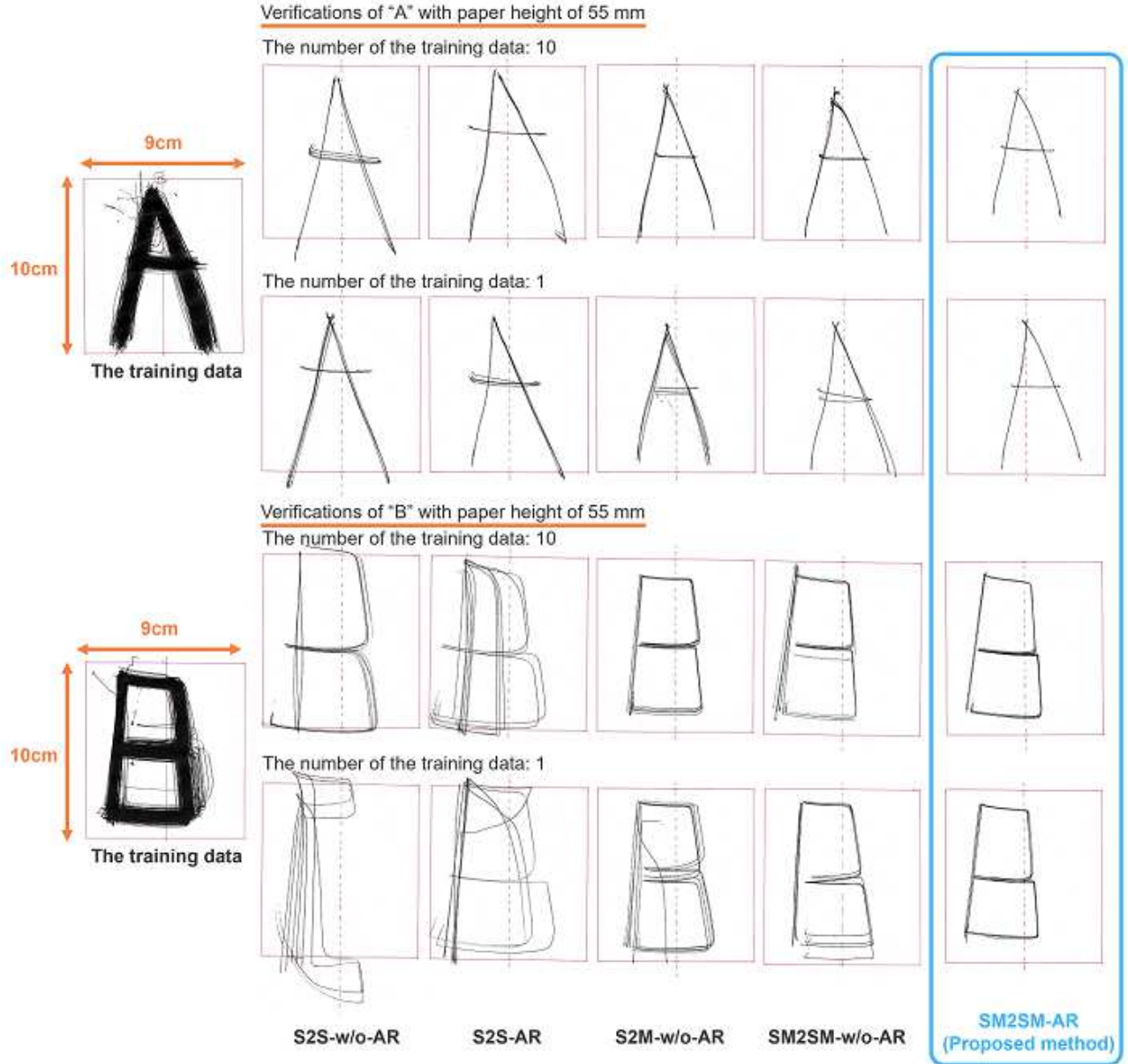


Fig. 13. The training data and the results of the writing task. The figures on the far left are the letters written by a human during the demonstrations. The letters of the training data appear to be thick because the letters were written on a single sheet of paper during all trials.

TABLE V
SUCCESS RATES OF THE WRITING TASK

Model	Success Rate [%]		
	Letter "A"	Letter "B"	Total
S2S-w/o-AR	0 (0/4)	0 (0/4)	0 (0/8)
S2S-AR	0 (0/4)	0 (0/4)	0 (0/8)
S2M-w/o-AR	75.0 (3/4)	75.0 (3/4)	75.0 (6/8)
SM2SM-w/o-AR	75.0 (3/4)	100 (4/4)	87.5 (7/8)
SM2SM-AR (proposed method)	100 (4/4)	100 (4/4)	100 (8/8)

high success rates. In addition, the robot could properly erase the line without stopping during all trials. The robot applied the appropriate force even at unlearned heights. Most of the failures were from moving slightly beyond the success area. Although none of the models exhibited a perfect performance because the definition of the success area was strictly set, the S2M and SM2SM models achieved an excellent performance in realizing fast motion while maintaining the proper force. Because this task was a reciprocating motion with a short cycle, a long-term prediction was not required, and it was a relatively easy task for bilateral control-based IL. Therefore, even the conventional S2M model without autoregressive learning showed as high a success rate as the proposed model. It was confirmed that the proposed method with autoregressive learning achieved an excellent performance even for a short-cycle task without adverse effects.

C. Experiment 3 (Writing letters)

1) *Task design*: A ballpoint pen was fixed to the slave. The goal of this task was to write the letters "A" and "B" on paper. Compared to the erasing task, this writing task was a long-term operation and required a correct long-term prediction. To succeed in this task, it was necessary to reproduce the proper force between the paper and pen. In addition, the robot had to reproduce the stroke order learned from the human demonstrations, that is, the ability to generate correct behavior based on the past and current state was necessary.

2) *Human demonstrations and dataset for learning*: We collected data with paper heights of 35, 55, and 75 mm. The letters "A" and "B" were collected as separate trials. Ten trials were conducted for each paper height. A total of 30 trials were conducted for each letter. One 20 s trial included motion required to write the same letter four times in a row. The letters are written inside the solid red line shown in Fig. 13. We wrote the letters such that the shape would be roughly the same during all trials without using any restraining tools including a ruler.

3) *Neural network architecture*: The NN model consisted of six LSTM layers, followed by a fully connected layer. A unit size of 50 was used for all layers. The mini-batch consisted of 100 random sets of 200 time-sequential samples corresponding to 4 s.

4) *Validation of the task*: In verifying the autonomous operation, the performance for paper heights of 55 and 65 mm was verified. In addition, verification was conducted for the cases in which 1 and 10 training data were used. Success was defined as the robot writing the letter five times continuously inside the solid red line shown in Fig. 13 with the correct stroke order. Verification was achieved for each

paper height and each number of training data. Therefore, four verifications were applied (two heights \times two training datasets).

5) *Experimental results*: The success rate of each model is shown in Table V. Only the proposed method was successful for all validations. The results of continuously writing the letter five times are shown in Fig. 13. In conventional methods, the trajectory of the letters was unstable every time. By contrast, with the proposed method, the letters were written in the same trajectory each time. In particular, in the case in which the training data were small in number, the difference with the other methods was noticeable. Only the proposed method could generate a trajectory with little fluctuation. This result indicated that the proposed method generated motion with little fluctuation in the long-term thanks to autoregressive learning *i.e.*, the model learned to minimize the total errors of the long-term prediction.

VI. CONCLUSION

In this study, we proposed a method of autoregressive learning for a bilateral control-based IL. Owing to the structure and autoregressive learning of the proposed model, the performance was improved compared to the conventional methods. During the experiments, three types of tasks were performed, and the proposed method had the highest success rate. In addition, the proposed method improved the generalization for unknown environments.

However, the proposed method had the point to be improved for the model structure. In the SM2SM model proposed in this paper, the master state predicted by the model in the previous step was input to the model during an autonomous operation. Therefore, the master state used in the input can be regarded as a virtual master state. If sudden environmental changes occur, this state of the virtual master is likely to differ from the state of the actual master. This error affects the model, and therefore, we will implement systems to correct the error to address this issue.

ACKNOWLEDGMENT

This work was supported by JST PRESTO Grant Number JPMJPR1755, Japan.

REFERENCES

- [1] R. Rahmatizadeh, P. Abolghasemi, L. Bölöi, and S. Levine, "Vision-based multi-task manipulation for inexpensive robots using end-to-end learning from demonstration," in *Proceedings of IEEE International Conference on Robotics and Automation (ICRA)*, pp. 3758–3765, 2018.
- [2] S. Levine, P. Pastor, A. Krizhevsky, and D. Quillen, "Learning hand-eye coordination for robotic grasping with deep learning and large-scale data collection," *The International Journal of Robotics Research*, vol. 37, no. 4–5, pp. 421–436, 2018.
- [3] T. Zhang, Z. McCarthy, O. Jow, D. Lee, X. Chen, K. Goldberg, and P. Abbeel, "Deep imitation learning for complex manipulation tasks from virtual reality teleoperation," in *Proceedings of IEEE International Conference on Robotics and Automation (ICRA)*, pp. 1–8, 2018.
- [4] P. Agrawal, A. Nair, P. Abbeel, J. Malik, S. Levine, "Learning to poke by poking: experiential learning of intuitive physics," in *Proceedings of Advances in neural information processing systems*, pp. 5074–5082, 2016.
- [5] H. Ravichandar, A. S. Polydoros, S. Chernova, and A. Billard, "Recent advances in robot learning from demonstration," *Annual Review of Control, Robotics, and Autonomous Systems*, vol. 3, pp. 297–330

- [6] B. Fang, S. Jia, D. Guo, M. Xu, S. Wen, and F. Sun, "Survey of imitation learning for robotic manipulation," *International Journal of Intelligent Robotics and Applications*, no. 3, pp. 362–369, 2019.
- [7] T. Yu, C. Finn, A. Xie, S. Dasari, T. Zhang, P. Abbeel, and S. Levine, "One-shot imitation from observing humans via domain-adaptive meta-learning," in *Proceedings of Robotics: Science and Systems (RSS)*, 2018.
- [8] D. Vogt, S. Stepputtis, S. Grehl, B. Jung, and H. B. Amor, "A system for learning continuous human-robot interactions from human-human demonstrations," in *Proceedings of IEEE International Conference on Robotics and Automation (ICRA)*, pp. 2882–2889, 2017.
- [9] P. C. Yang, K. Sasaki, K. Suzuki, K. Kase, S. Sugano, and T. Ogata, "Repeatable folding task by humanoid robot worker using deep learning," *IEEE Robotics and Automation Letters*, vol. 2, no. 2, pp. 397–403, 2017.
- [10] A. Gupta, V. Kumar, C. Lynch, S. Levine, and K. Hausman, "Relay policy learning: Solving long-horizon tasks via imitation and reinforcement learning," [arXiv:1910.11956](https://arxiv.org/abs/1910.11956), 2019.
- [11] P. Kormushev, S. Calinon, and D. G. Caldwell, "Imitation learning of positional and force skills demonstrated via kinesthetic teaching and haptic input," *Advanced Robotics*, vol. 25, no. 5, pp. 581–603, 2011.
- [12] L. Rozo, P. Jiménez, and C. Torras, "A robot learning from demonstration framework to perform force-based manipulation tasks," *Intel Serv Robotics*, vol. 6, no. 1, pp. 33–51, 2013.
- [13] L. Rozo, D. Bruno, S. Calinon, and D. G. Caldwell, "Learning optimal controllers in human-robot cooperative transportation tasks with position and force constraints," in *Proceedings of IEEE/RSJ International Conference on Intelligent Robots and Systems (IROS)*, pp. 1024–1030, 2015.
- [14] A. X. Lee, H. Lu, A. Gupta, S. Levine, and P. Abbeel, "Learning force-based manipulation of deformable objects from multiple demonstrations," in *Proceedings of IEEE International Conference on Robotics and Automation (ICRA)*, pp. 177–184, 2015.
- [15] H. Ochi, W. Wan, Y. Yang, N. Yamanobe, J. Pan, and K. Harada, "Deep learning scooping motion using bilateral teleoperations," in *Proceedings of 2018 3rd International Conference on Advanced Robotics and Mechatronics (ICARM)*, pp. 118–123, 2018.
- [16] P. Kormushev, D. N. Nenchev, S. Calinon, and D. G. Caldwell, "Upper-body kinesthetic teaching of a free-standing humanoid robot," in *Proceedings of IEEE International Conference on Robotics and Automation (ICRA)*, pp. 3970–3975, 2011.
- [17] M. Tykal, A. Montebelli, and V. Kyrki, "Incrementally assisted kinesthetic teaching for programming by demonstration," in *Proceedings of 2016 11th ACM/IEEE International Conference on Human-Robot Interaction (HRI)*, pp. 205–212, 2016.
- [18] T. Adachi, K. Fujimoto, S. Sakaino, and T. Tsuji, "Imitation learning for object manipulation based on position/force information using bilateral control," in *Proceedings of IEEE/RSJ International Conference on Intelligent Robots and Systems (IROS)*, pp. 3648–3653, 2018.
- [19] A. Sasagawa, K. Fujimoto, S. Sakaino, and T. Tsuji, "Imitation learning based on bilateral control for human-robot cooperation," *IEEE Robotics and Automation Letters*, vol. 5, no. 4, pp. 6169–6176, 2020.
- [20] S. Sakaino, T. Sato, and K. Ohnishi, "Multi-DOF micro-macro bilateral controller using oblique coordinate control," *IEEE Transactions on Industrial Informatics*, vol. 7, no. 3, pp. 446–454, 2011.
- [21] T. Kitamura, N. Mizukami, H. Mizoguchi, S. Sakaino, and T. Tsuji, "Bilateral control in the vertical direction using functional electrical stimulation," *IEEE Journal of Industry Applications*, vol. 5, no. 5, pp. 398–404, 2016.
- [22] S. Hochreiter and J. Schmidhuber, "Long short-term memory," *Neural Computation*, vol. 9, no. 8, pp. 1735–1780, 1997.
- [23] R. J. Williams and D. Zipser, "A learning algorithm for continually running fully recurrent neural networks," *Neural computation*, vol. 1, no. 2, pp. 270–280, 1989.
- [24] A. Lamb, A. Goyal, Y. Zhang, S. Zhang, A. Courville, and Y. Bengio, "Professor forcing: A new algorithm for training recurrent networks," *Advances in neural information processing systems*, pp. 4601–4609, 2016.
- [25] K. Kase, R. Nakajo, H. Mori, and T. Ogata, "Learning multiple sensorimotor units to complete compound tasks using an RNN with multiple attractors," in *Proceedings of IEEE/RSJ International Conference on Intelligent Robots and Systems (IROS)*, 2019.
- [26] W. Iida and K. Ohnishi, "Reproducibility and operability in bilateral teleoperation," in *Proceedings of the IEEE International Workshop on Advanced Motion Control*, pp. 217–222, 2004.
- [27] K. Tanida, T. Okano, T. Murakami, and K. Ohnishi, "Control structure determination of bilateral system based on reproducibility and operability," *IEEE Journal of Industry Applications*, vol. 8, no. 5, pp. 767–778, 2019.
- [28] K. Ohnishi, M. Shibata, and T. Murakami, "Motion control for advanced mechatronics," *IEEE/ASME Transaction on Mechatronics*, vol. 1, no. 1, pp. 56–67, 1996.
- [29] T. Murakami, F. Yu, and K. Ohnishi, "Torque sensorless control in multidegree-of-freedom manipulator," *IEEE Transactions on Industrial Electronics*, vol. 40, no. 2, pp. 259–265, 1993.
- [30] T. Yamazaki, S. Sakaino, and T. Tsuji, "Estimation and kinetic modeling of human arm using wearable robot arm," *Electrical Engineering in Japan*, vol. 199, no. 3, pp. 57–67, 2017.
- [31] S. Bengio, O. Vinyals, N. Jaitly, and N. Shazeer, "Scheduled sampling for sequence prediction with recurrent neural networks," *Advances in Neural Information Processing Systems*, Vol. 1, pp. 1171–1179, 2015.
- [32] W. Zhang, Y. Feng, F. Meng, D. You, and Q. Liu, "Bridging the gap between training and inference for neural machine translation," in *Proceedings of the 57th Annual Meeting of the Association for Computational Linguistics*, pp. 4334–4343, 2019.
- [33] Y. Xu, K. Zhang, H. Dong, Y. Sun, W. Zhao, and Z. Tu, "Rethinking exposure bias in language modeling," [arXiv:1910.11235](https://arxiv.org/abs/1910.11235), 2019.